Permian volcanism in the Mongolian Orogenic Zone, northeast China: Geochemistry, magma sources and petrogenesis

Article *in* Geological Magazine · March 2001

DOI: 10.1017/S0016756801005210

6 authors, including:

Yongfeng Zhu
Peking University
158 PUBLICATIONS **2,627** CITATIONS

SEE PROFILE

Permian volcanism in the Mongolian orogenic zone, northeast China: geochemistry, magma sources and petrogenesis

YONGFENG ZHU*‡§, SHIHUA SUN†, LIBING GU*, YOSHIHIDE OGASAWARA‡, NENG JIANG† & HIROJI HONMA†

*Department of Geology, Peking University, Beijing 100871, China
†Institute of Geology and Geophysics, Chinese Academy of Sciences, Beijing 100029, China
‡Department of Earth Sciences, Waseda University, Tokyo 169-50, Japan

(*Received* 20 September 2000; *accepted* 5 December 2000)

Abstract – Lower Permian volcanism was the first magmatic activity to occur after the collision events in the Mongolian orogenic zone, east China. The Permian volcanic rocks are therefore a key to understanding the dynamics of the unified continental lithosphere. The volcanic rocks consist of basic and intermediate rocks. The intermediate rocks with high initial $^{87}Sr/^{86}Sr$ ratios (0.7051 to 0.7052) and low ε_{Nd} values (–0.73 to –3.57) generally overlie the basic rocks in the field. The basic rocks have relatively low initial $^{87}Sr/^{86}Sr$ ratios (0.7034 to 0.7051) and high ε_{Nd} values (2.72 to –0.10). Two parallel Rb–Sr isochrons give almost the same age, about 270 Ma. One consists of the basic rocks giving an initial isochron $^{87}Sr/^{86}Sr$ ratio of 0.7035. The other consists of the intermediate rocks and one sample of basalt, which give an initial isochron $^{87}Sr/^{86}Sr$ value of 0.7051. The strong correlations between SiO_2 and other major elements suggest that fractional crystallization played an important role in the magmatic processes. However, fractional crystallization cannot explain the geochemistry of most incompatible trace elements and Sr–Nd isotope characteristics. The positive correlation between Th/Nb and $(La/Sm)_N$ ratios demonstrates the direct relation between the enrichment of the light rare earth elements and the contamination of continental sediments. The high contents of large ion lithosphere elements (LILE) in the Permian volcanic rocks may suggest an additional 'crust + fluid' component, especially in the intermediate rocks, which are highly enriched in Ba (> 400 ppm) relative to the basic rocks (< 200 ppm). We propose that the subduction slab dropped into depleted mantle and released fluid, which induced the mantle metasomatism and LILE enrichment. The metasomatized mantle partially melted and formed the 'primary' magma. This primary magma assimilated with the Proterozoic biotite–quartz schist during its rise, and finally formed the Permian volcanic rocks. Magma assimilated with the Proterozoic biotite–quartz schist in small amounts could have produced the basic rocks, while assimilation of larger amounts of magma (because of longer assimilation time) would generate intermediate rocks.

1. Introduction

In the recent literature, many authors suggest that the geochemistry of post-collisional magmatic rocks reflects the composition of their source materials (e.g. Liegeois *et al.* 1998). In this respect the source of post-collisional magmatism commonly contains a large number of components including middle ocean ridge basalts (MORB), ocean island basalts (OIB), subduction sediments, oceanic and continental crust (e.g. Coulon & Thorpe, 1981; Di Vincenzo & Rocchi, 1999). Unravelling the complexity of the post-collisional magma requires precise knowledge of the nature of the magma source (Liegeois, 1998).

The Mongolian orogenic belt is considered to be a series of late Precambrian to early Mesozoic suture zones between the Siberian craton and the north China craton, which has evolved through accretionary tectonics (Sengor, Natal'in & Burtman, 1993; Zorin, Belichenko & Turutano, 1993). It consists of two main parts (Sengor & Natal'in, 1996): the Altaids in the north and the Manchurides in the south (Fig. 1a). The Manchurides consist of two parallel fold belts: the belts formed during the Devonian–Carboniferous period are distributed symmetrically along the rim; the belt formed during the Carboniferous–Permian period is located in the centre (Fig. 1b). This characteristic demonstrates that new continental material was accreted to the north margin of the north China craton and to the south margin of the Altaids symmetrically. The belt formed during the Carboniferous–Permian period is the last record in the Mongolian orogenic belt. Two ophiolite belts recorded the last subduction process (Tang, 1990; Robinson *et al.* 1999) that occurred in the eastern part of the Manchurides (Fig. 1b): the Xilamulun ophiolite in the south and Hegenshan ophiolite in the north. The Hegenshan ophiolite yielded a date of 430 Ma (Rb–Sr isochron age: Hsu, Wang & Hao, 1991). Both of these ophiolites are covered by Permian to Jurassic volcanic–sedimentary rocks.

Numerous studies have focused on documenting the tectonic evolution of this region (e.g. Tang, 1990;

§Author for correspondence: yongfeng@eyou.com

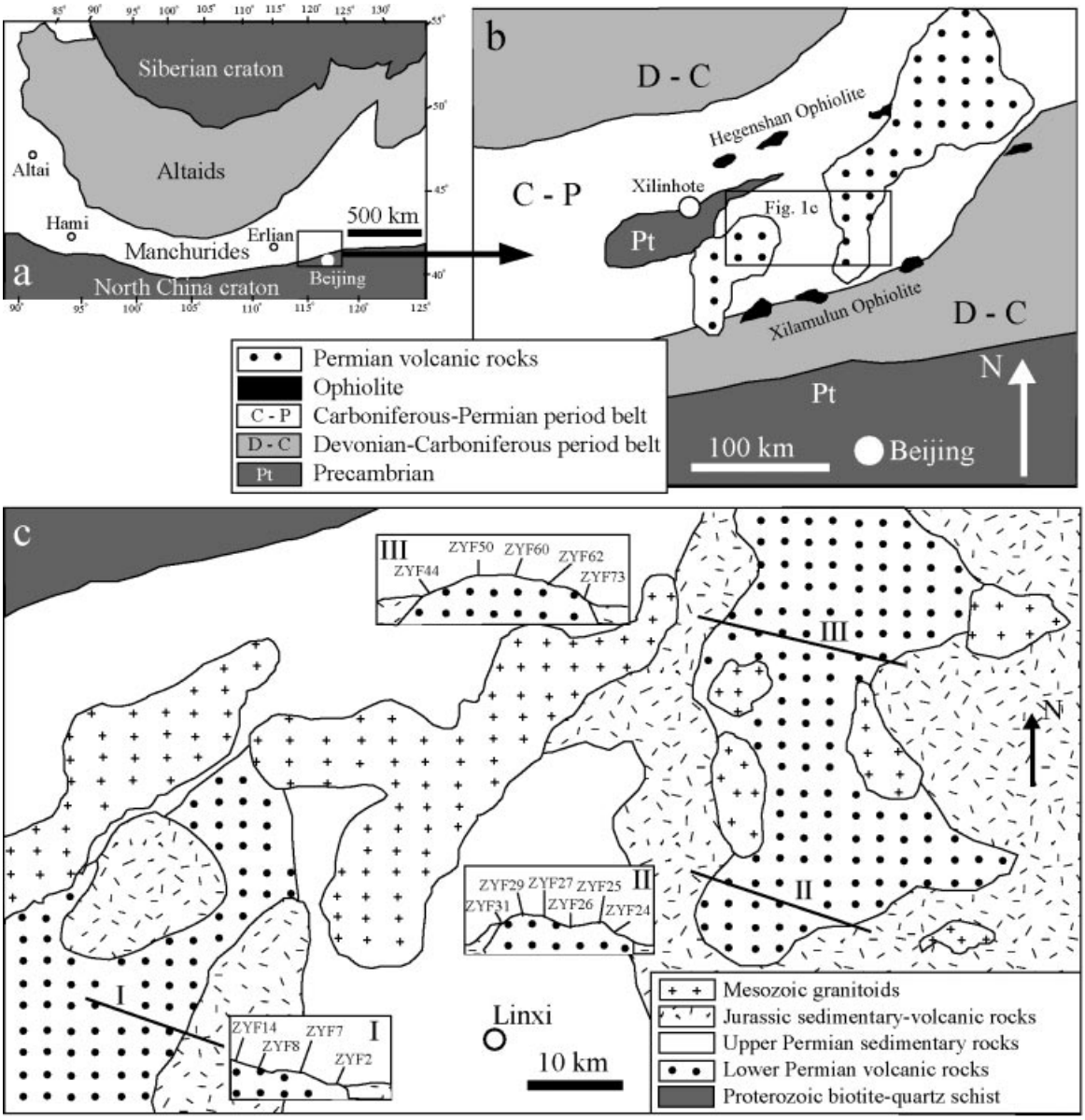

Figure 1. (a) Tectonic setting of the Mongolian orogenic belt (modified from Sengor & Natal'in, 1996). The Altaids are mainly composed of Early Palaeozoic rocks; the Manchurides mainly consist of Late Palaeozoic rocks. (b) Southeastern part of the Manchurides where Permian volcanic rocks occur (modified from Shao, 1991). (c) Geological map of the studied area; insets (I, II and III) show field sections where numbered samples were collected.

Shao, 1991). They have demonstrated that during Early Palaeozoic times, an ocean existed between the north China and Siberian cratons, and was subsequentially subducted under the continental mantle, finally leading to collision of the two cratons. The Lower Permian volcanism was the first magmatic activity to occur after the collision events in this area. The Permian volcanic rocks, therefore, are a key to understanding the dynamics of the unified continental lithosphere. Here we report Nd–Sr isotopic, major and trace element geochemical data for the Permian volcanic rocks and discuss their petrogenesis and magma sources.

2. Petrography

The oldest rocks exposed in the studied area are Proterozoic metamorphic rocks, which belong to the Baoyintu formation of the Xilinhote complex (Fig. 1b), mainly consisting of quartzite, biotite–quartz schist and biotite–plagioclase gneiss with plagioclase amphibolite locally. A Sm–Nd isochron for the amphibolite (with $\varepsilon_{Nd} = +6$) as well as for the biotite–quartz schist (with $\varepsilon_{Nd} = -11$) yields 1.2 Ga (Zhu *et al.* unpub. data). The Lower Permian volcanic– sedimentary formation (consisting of tuff, lavas and volcaniclastics) and Upper Permian sedimentary formation (mainly

sandstone, siltstone and slate) directly overlie the metamorphic rocks. A Jurassic volcanic–sedimentary formation overlies the Permian sedimentary rocks. Mesozoic magma intruded into all these units (Fig. 1c).

The thickness of the Lower Permian volcanic–sedimentary formation varies from about 500 m to 1200 m, and is mainly composed of volcanic rocks. Only volcanic rocks (lava) from this formation are studied here. The rock sequence is similar in different outcrops (sections I and III in Fig. 1c): the intermediate rocks generally overlie the basic rocks although the boundary between them is not clear in the field. In one outcrop (section II) only basic rocks occur (sample ZYF24-31). Samples ZYF8, ZYF24 and ZYF50 are taken from cores of pillow basalts. All these volcanic rocks are slightly altered, mainly in the groundmass. Most phenocrysts are rather fresh. Basic rocks have 15 to 40 vol.% phenocrysts of diopside, plagioclase and rarely olivine. Subhedral plagioclase phenocrysts were partially resorbed and filled by groundmass. The groundmass is composed of fine-grained plagioclase, pyroxene, amphibole and magnetite. The intermediate rocks have phenocrysts of plagioclase (5–25 vol.%) and green amphibole (3–10 vol.%). Subhedral plagioclase phenocrysts were partly resorbed. The groundmass consists mostly of fine-grained plagioclase laths, amphibolite and magnetite in pale devitrified glass.

3. Analytical techniques

Whole rocks of the representative samples were ground in an agate mill, after careful washing in distilled water. Major elements were measured by XRF spectrometer on glass disks made by fusion of whole rock with lithium metaborate. Trace elements were analysed by inductively coupled plasma-mass spectrometry (ICP-MS) at the Research Center for Mineral and Resource Exploration (RCMRE), Chinese Academy of Sciences. Precision is 0.5% for major element oxides and variable in the range ~2–5% for trace elements of higher than 100 ppm, ~2–10% for trace elements of ~20–100 ppm, and ~5–20% for trace element contents of lower than 20 ppm. Analytical data are given in Table 1.

Whole rock samples were analysed for Sr and Nd isotopic compositions at the Research Center for Mineral and Resource Exploration. Strontium and neodymium were extracted by conventional ion exchange chromatographic techniques, after dissolution with a HF–HNO_3–HCl mixture in a closed Teflon bottle at 120 °C for 72 h. Sr and Nd isotopic ratios were measured using a Finnigan MAT 262 multiple-collector mass spectrometer, thermal ionization mass spectrometer running in dynamic mode. Replicate analyses of the NBS-987 reference standard gave average values of 0.710287 ± 0.000010 ($n = 14$) (all errors and standard deviations are given at the 2σ confidence level). $^{87}Sr/^{86}Sr$ was normalized within-run to $^{86}Sr/^{88}Sr = 0.1194$. The $^{143}Nd/^{144}Nd$ ratio was normalized within-run to $^{146}Nd/^{144}Nd = 0.7219$. The Nd La Jolla standard yielded an average ratio of $^{143}Nd/^{144}Nd = 0.511942 \pm 0.000012$ ($n = 12$). Blanks were on the order of < 0.3 ng for Sr and < 0.05 ng for Nd. Replicate analyses gave an external reproducibility better than 2% for Rb–Sr and 0.2% for Sm–Nd. Rb–Sr isochron ages are calculated by using the program Isoplot/Ex2.3 (Ludwig, 2000). The Nd–Sr isotopic compositions of the Permian volcanic rocks are given in Table 1.

4. Element geochemistry

The Permian volcanic rocks are classified as basalt, basaltic andesite, basaltic trachy-andesite and trachy-andesite (Fig. 2a) according to Le Maitre *et al.* (1989). Most rocks belong to the medium-K group (Fig. 2b). The basic rocks (basalt and basaltic andesite) have lower Al_2O_3, Na_2O, P_2O_5 and TiO_2 contents (Fig. 2c–f, respectively) and higher Fe_2O_3, MgO, CaO contents (Fig. 2g–i, respectively) relative to the intermediate rocks (basaltic trachy-andesite and trachy-andesite). The contents of major elements in the basic rocks vary greatly relative to the intermediate rocks. A reverse correlation is shown for MgO and K_2O+Na_2O (Fig. 2j). These observations suggest that magmatic differentiation is probably responsible for the varying contents of major elements. This is confirmed by the correlation between major elements and Mg no. shown in Figure 3. The Mg no. is negatively correlated with Al_2O_3 (Fig. 3a) and TiO_2 (Fig. 3b), but positively with CaO (Fig. 3c) and Fe_2O_3 (Fig. 3d).

The compatible trace elements such as Cr, Ni, Co and V tend to partition into mineral phases during magma crystallization. Their concentrations will decrease during fractional crystallization. The crystallization and fractionation of olivine is the main factor controlling Ni concentration in magma. Similarly, the content of V is controlled by pyroxene and magnetite; Cr and Co are controlled mainly by olivine and diopside. All these trace elements have good correlation with SiO_2 and show a general differentiation trend from the basic to intermediate rocks (Fig. 3e–h). This trend is consistent with the differentiation trend demonstrated by the major elements (Figs 2, 3a–d) involving diopside and amphibole.

Rare earth elements (REE) are regarded as among the least soluble trace elements and are relatively immobile during low-temperature metamorphism, weathering and hydrothermal alteration. Therefore, REE patterns even in slightly altered rocks can represent the original composition of the unaltered parent (Rollinson, 1993). REE abundance varies greatly in the Permian volcanic rocks (total REE from 36 to 127 ppm, Table 1). The basic rocks have lower REE contents than the intermediate rocks. The chondrite-normalized REE patterns of the Permian volcanic

Table 1. Chemical composition of volcanic rocks from Inner Mongolia, North China

Sample no.	ZYF2	ZYF7	ZYF8	ZYF14	ZYF24	ZYF25	ZYF26	ZYF27	ZYF29	ZYF31	ZYF44	ZYF50	ZYF60	ZYF62	ZYF73	PBQS
Rock	CHA	Basalt	BA	Basalt	Basalt	Basalt	Basalt	Basalt	Basalt	Basalt	Basalt	BCHA	CHA	CHA	CHA	Schist
SiO_2	59.13	50.98	53.95	47.98	47.61	50.11	48.23	48.82	50.42	48.65	50.08	57.17	60.24	59.44	61.30	69.01
TiO_2	1.12	0.85	0.91	0.58	0.63	0.72	0.56	0.63	0.62	0.53	0.82	1.05	1.16	1.12	1.21	0.64
Al_2O_3	16.01	12.91	14.01	10.04	10.15	12.46	9.78	10.81	12.55	11.12	12.87	16.25	16.28	17.19	16.96	12.19
Fe_2O_3	7.65	10.14	10.08	12.17	12.14	10.52	11.64	11.01	10.22	10.13	10.49	7.92	6.52	7.12	6.24	3.82
MnO	0.14	0.18	0.18	0.28	0.22	0.17	0.21	0.22	0.13	0.21	0.17	0.13	0.1	0.09	0.23	0.19
MgO	2.91	9.58	7.35	12.46	12.77	11.13	12.62	12.42	11.74	12.91	10.63	3.42	2.94	2.09	2.35	2.45
CaO	4.67	10.17	6.83	14.05	14.11	11.31	14.41	13.33	10.64	14.35	9.88	6.02	4.27	3.77	3.31	8.35
Na_2O	4.32	2.16	3.14	1.01	0.82	1.73	0.69	1.03	1.84	0.61	2.03	4.13	4.13	4.22	4.29	1.42
K_2O	2.34	1.23	1.61	0.42	0.45	0.75	0.39	0.52	0.69	0.36	0.95	1.68	2.73	2.96	2.74	1.93
P_2O_5	0.28	0.20	0.22	0.15	0.16	0.19	0.15	0.16	0.19	0.14	0.17	0.24	0.29	0.28	0.32	0.17
LOI	1.32	0.94	1.21	0.48	0.78	0.84	0.95	0.77	1.02	0.53	1.27	1.23	0.79	1.31	0.88	0.15
Total	99.89	99.34	99.49	99.62	99.71	99.93	99.63	99.72	100.06	99.54	99.36	99.24	99.45	99.59	99.83	100.32
Cs	1.19	1.34	0.81	0.33	2.00	4.87	0.46	2.23	4.63	0.56	6.04	0.88	0.97	4.76	5.10	4.10
Rb	27.21	22.55	25.27	7.76	14.50	67.37	5.44	24.10	20.43	5.76	73.59	36.94	59.39	75.13	63.85	85.62
Sr	384.4	339.7	208.3	220.5	220.3	293.0	356.6	243.8	253.1	469.7	278.5	649.9	579.8	158.8	248.7	99.90
Ba	588.4	191.2	204.4	173.0	64.02	133.7	60.89	113.3	198.5	136.4	89.4	432.8	731.6	460.7	627.2	451.1
Th	1.74	1.56	1.08	1.27	0.95	0.89	0.77	0.79	1.30	0.87	0.48	3.27	3.30	1.48	1.71	8.20
U	1.09	0.37	0.36	0.52	0.34	0.23	0.34	0.34	0.37	0.31	0.15	1.01	1.30	0.86	1.01	4.13
Nb	9.67	5.07	4.49	3.29	5.08	5.86	3.37	2.22	4.30	3.71	3.49	9.03	9.23	8.90	11.73	13.80
Zr	211.1	44.16	95.37	56.87	33.45	84.36	26.51	35.59	57.30	26.88	81.10	212.7	234.1	125.3	171.3	188.0
Y	19.04	17.19	20.54	12.97	11.78	20.27	11.01	10.68	13.22	10.33	19.51	20.99	26.01	20.12	24.64	30.51
Cr*	131.1	330.4	172.0	815.1	727.1	347.1	704.3	775.0	516.2	554.1	350.0	69.0	89.2	61.1	48.0	29.1
Ni*	42.3	93.8	85.3	255.6	300.3	194.5	248.6	289.0	216.1	239.8	184.5	46.1	42.8	16.9	12.5	28.9
V*	122.6	211.1	214.1	215.4	240.2	221.2	225.2	217.2	233.3	220.6	234.3	176.4	128.4	133.6	131.9	82.2
Co	27.80	53.02	32.28	72.54	66.82	55.47	71.84	64.49	61.70	60.40	41.33	31.65	21.92	23.36	10.39	16.15
Sc	12.28	33.29	18.71	33.32	38.56	25.23	35.43	28.19	35.7	33.54	28.00	19.01	16.58	9.09	16.38	11.21
La	17.71	8.18	6.58	6.70	6.80	7.69	5.48	5.73	7.41	5.58	7.28	21.98	21.29	11.73	19.56	23.78
Ce	37.35	19.22	17.43	14.81	14.41	18.82	11.84	11.27	15.87	11.55	18.55	46.64	39.98	20.42	50.04	58.10
Pr	4.54	2.67	2.52	2.12	2.07	2.92	1.73	1.81	2.05	1.71	2.84	6.42	5.76	2.08	6.13	6.05
Nd	15.29	10.39	11.33	8.56	8.27	11.19	6.92	6.98	8.20	6.68	11.03	23.67	25.01	7.57	25.10	21.12
Sm	3.68	3.20	3.71	2.49	2.38	3.51	2.18	2.15	2.18	2.00	3.58	5.46	6.21	2.23	6.00	4.83
Eu	0.95	1.03	1.33	1.00	1.10	1.27	0.72	1.01	0.81	0.75	1.27	1.65	1.91	0.62	1.53	0.81
Gd	3.36	3.57	4.53	2.80	2.57	4.02	2.29	2.46	2.39	2.25	4.10	5.24	6.27	2.72	5.19	5.18
Tb	0.58	0.56	0.81	0.45	0.40	0.66	0.37	0.38	0.40	0.36	0.66	0.78	0.94	0.49	0.90	0.91
Dy	3.53	3.40	5.17	2.66	2.29	3.99	2.16	2.07	2.05	2.07	4.01	4.36	5.19	3.32	5.10	5.42
Ho	0.73	0.66	1.13	0.53	0.45	0.82	0.41	0.42	0.43	0.41	0.80	0.82	0.99	0.70	0.98	1.10
Er	1.99	1.86	3.16	1.49	1.26	2.31	1.21	1.20	1.21	1.16	2.23	2.28	2.75	2.17	2.83	3.31
Tm	0.30	0.27	0.45	0.21	0.17	0.33	0.17	0.17	0.18	0.17	0.32	0.32	0.39	0.32	0.43	0.50
Yb	2.17	1.79	2.59	1.41	1.17	2.11	1.13	1.08	1.01	1.05	2.04	2.02	2.47	2.29	2.86	3.27
Lu	0.35	0.28	0.39	0.22	0.18	0.33	0.18	0.17	0.18	0.17	0.30	0.32	0.39	0.36	0.49	0.51
SREE	92.54	57.09	61.13	45.44	43.53	59.98	36.79	36.89	44.37	35.91	59.00	121.95	119.55	57.02	127.13	134.90
d Eu	0.83	0.93	0.99	1.16	1.36	1.04	0.99	1.34	1.08	1.08	1.02	0.94	0.94	0.77	0.84	0.50
$(La/Yb)_N$	5.84	3.28	1.82	3.42	4.16	2.62	3.46	3.81	5.27	3.82	2.56	7.82	6.19	3.68	4.91	5.22
$(Gd/Yb)_N$	1.27	1.65	1.45	1.64	1.81	1.58	1.67	1.89	1.95	1.77	1.66	2.15	2.1	0.98	1.5	1.14
$^{87}Rb/^{86}Sr$	0.205	0.192	0.351	0.102	0.190	0.495	0.044	0.286	0.233	0.035	0.764	0.164	0.296	1.367	0.742	2.477
$^{87}Sr/^{86}Sr$	0.705920	0.704170	0.704824	0.705504	0.704213	0.705781	0.703647	0.704637	0.704420	0.703615	0.706421	0.705730	0.706311	0.708001	0.708011	0.718470
2s error	0.000011	0.000010	0.000011	0.000009	0.000010	0.000015	0.000008	0.000012	0.000011	0.000008	0.000015	0.000009	0.000012	0.000014	0.000016	0.000016
$^{87}Sr/^{86}Sr$ (T)	0.705133	0.703432	0.703476	0.705112	0.703483	0.703880	0.703478	0.703538	0.703525	0.703481	0.703486	0.705100	0.705174	0.702750	0.705161	0.714247
$^{147}Sm/^{144}Nd$	0.146	0.186	0.198	0.176	0.174	0.190	0.190	0.186	0.161	0.181	0.196	0.139	0.150	0.178	0.145	0.138
$^{143}Nd/^{144}Nd$	0.512591	0.512651	0.512708	0.512701	0.512734	0.512664	0.512761	0.512687	0.512701	0.512805	0.512714	0.512691	0.512683	0.512614	0.512547	0.512521
2s error	0.000008	0.000010	0.000014	0.000009	0.000009	0.000009	0.000010	0.000011	0.000012	0.000009	0.000012	0.000009	0.000008	0.000010	0.000009	0.000009
Nd (T)	–2.68	–0.10	1.41	0.51	1.09	0.26	2.18	0.59	–0.01	2.72	1.47	–0.94	–0.73	–1.11	–3.57	–11.20

BA = basaltic andesite, BCHA = basaltic trachy-andesite, CHA = trachy-andesite, PBQS = representative Proterozoic biotite-quartz schist
* Major elements and Cr, Ni, V were measured by XRF, all other trace elements by ICP-MS. Oxides in wt %, trace elements in ppm.

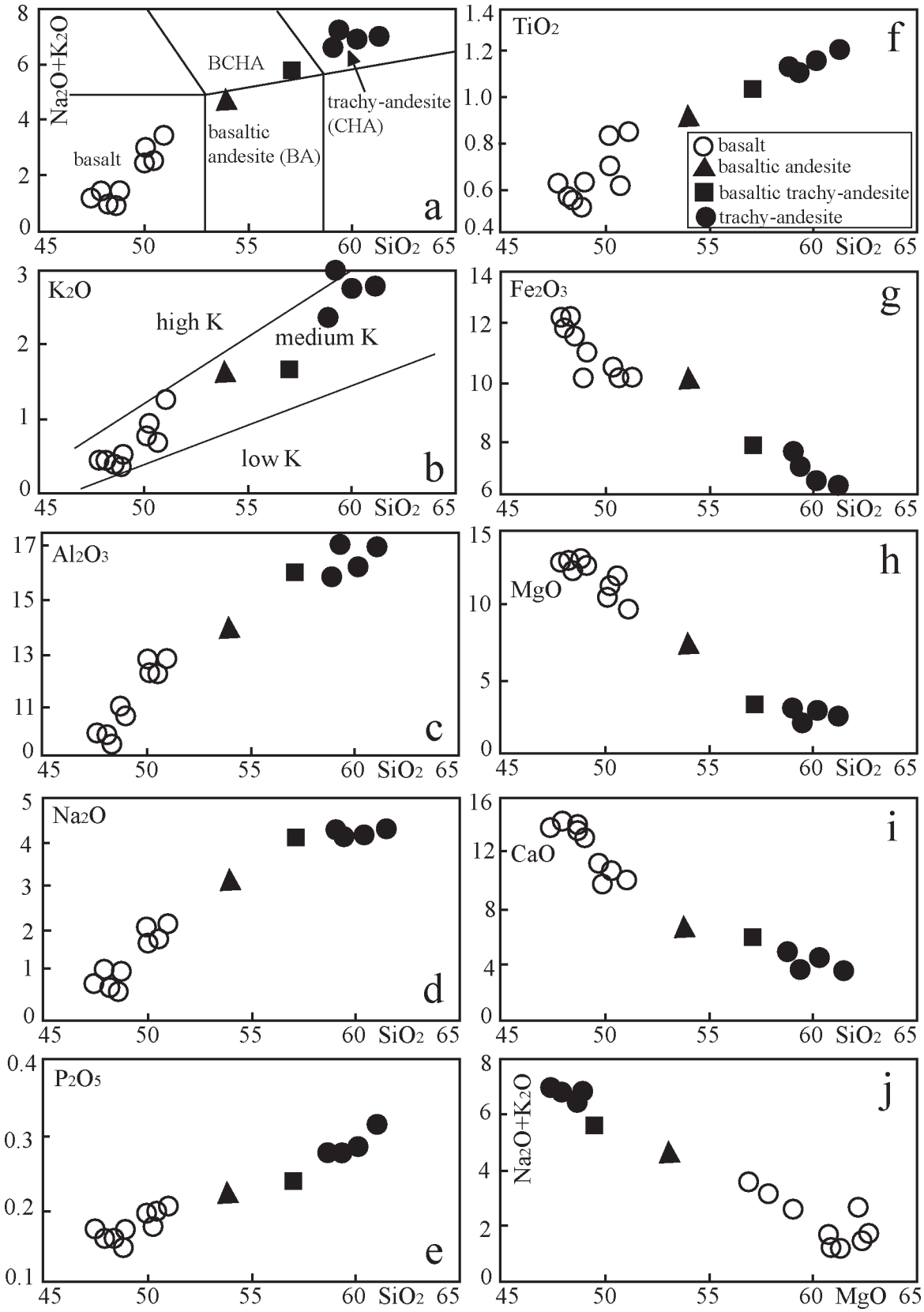

Figure 2. (a) Permian volcanic rocks are classified as basalt, basaltic andesite (BA), basaltic trachy-andesite (BCHA) and trachy-andesite (CHA) according to Le Maitre *et al.* (1989). Most rocks belong to the medium-K group on the diagram SiO_2 vs. K_2O (b). Samples formed rough differentiation trends from basic to intermediate rocks for all major elements (c–i). A reverse correlation is shown in the diagram of MgO vs. K_2O+Na_2O (j). All units for oxides are wt %.

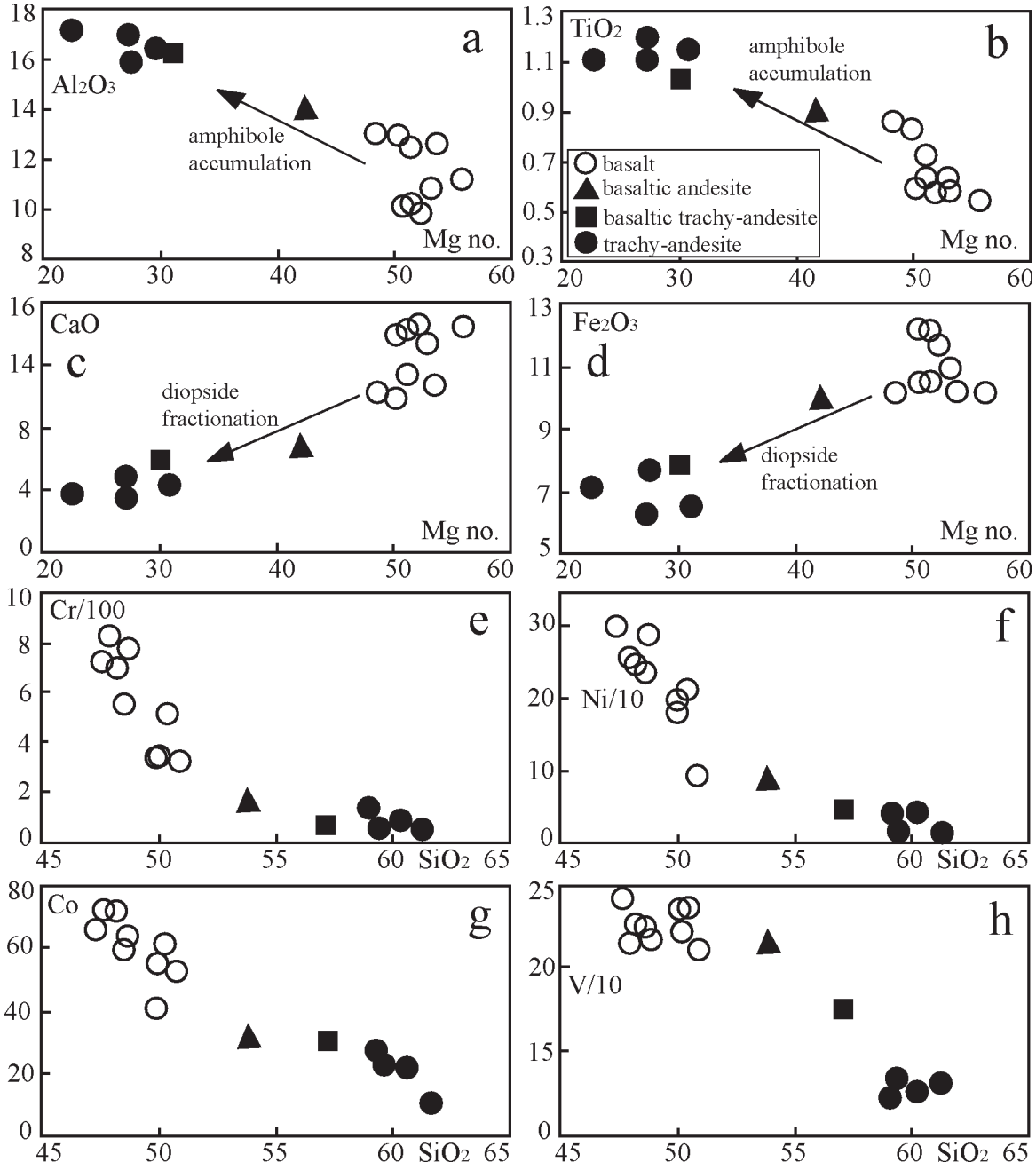

Figure 3. (a–d) Correlations between Mg no. and selected major elements showing fractional crystallization trend; all units for oxides are wt%. (e–h) General differentiation trend from the basic to intermediate rocks formed in the plots of some selected compatible trace elements (ppm) vs. SiO_2 (wt%).

rocks are largely variable depending on rock types. Basalts have slightly light REE (LREE)-enriched patterns with some positive Eu anomalies (Fig. 4a). Basaltic andesite has an almost flat REE pattern (Fig. 4b). However, basaltic trachy-andesite has a strong LREE-enriched pattern with no Eu anomaly (Fig. 4b). Trachy-andesite has LREE-enriched patterns with negative Eu anomalies (Fig. 4c). In general, the intermediate rocks are strongly LREE enriched (with $(La/Yb)_N$ = 3.68–7.82, Table 1) with negative Eu anomalies (δEu = 0.77–0.94, Table 1). The basic rocks, however, are slightly enriched in LREE (with $(La/Yb)_N$ = 1.82–5.27, Table 1) without Eu anomalies or with positive Eu anomalies (δEu of 0.93–1.34, Table 1).

In primitive mantle-normalized diagrams, basalts show enrichments of Cs, Rb, Ba, U, K and Sr, and depletions of Th, Nb, Zr and Ti (Fig. 5a). Similarly to basalts, basaltic andesite is enriched in Cs, Rb, Ba, U and K, and depleted in Th, Nb and Ti (Fig. 5b). Basaltic trachy-andesite, however, shows much higher enrichments of Cs, Rb, Ba, U, K and light REE with lower enrichments of Th, Nb and Ti (Fig. 5b). Trachy-

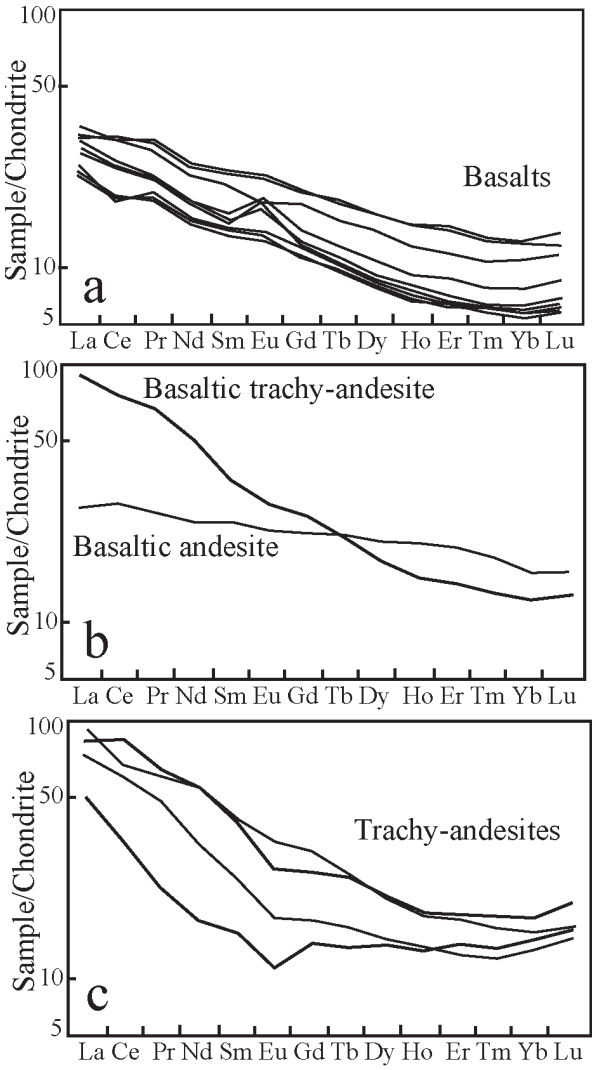

Figure 4. Chondrite-normalized REE distribution patterns for basalts (a), basaltic trachy-andesite and basaltic andesite (b) and trachy-andesites (c).

andesite shows strong enrichments of almost all incompatible trace elements, with the exceptions of Th and Nb (Fig. 5c). The abundances of the trace elements in the Permian volcanic rocks are much higher than in primitive mantle. However, almost all samples are enriched in Nb and LILE, but depleted in Ce in the enriched MORB (E-MORB) normalized diagrams (Fig. 5d–f). Basalts show obvious enrichments of Cs, Rb, Ba, Nb and Sm relative to the E-MORB (Fig. 5d); basaltic andesite and basaltic trachy-andesite are enriched in Cs, Rb, Ba and Nb with obvious Th enrichment only in basaltic trachy-andesite (Fig. 5e). The trachy-andesites show strong Cs, Rb, Ba, Th, K and Nb enrichments relative to E-MORB (Fig. 5f). Comparing Figure 5a–c with Figure 5d–f, it is clear that the trace element abundances in the Permian volcanic rocks are more similar to E-MORB than to the primitive mantle.

5. Nd–Sr isotopic geochemistry

Isotope compositions of strontium and neodymium in samples representative of the Permian volcanic rocks are reported in Table 1. Two parallel isochrons can be determined in the plot of the measured $^{87}Sr/^{86}Sr$ and $^{87}Rb/^{86}Sr$ values (Fig. 6a). The intermediate rocks and one sample of the basalt (ZYF14) form a Rb–Sr isochron, giving an age of 277 ± 15 Ma and an initial $^{87}Sr/^{86}Sr$ value of 0.705107 ± 0.000066 (MSWD = 5.2). The basic rocks form another Rb–Sr isochron giving an age of 272 ± 11 Ma with an initial $^{87}Sr/^{86}Sr$ value of 0.703481 ± 0.000048 (MSWD = 10.8). These two age values are similar within their error limits. Two samples (ZYF25 and ZYF62) do not fit the isochrons (Fig. 6a). The extremely high $^{87}Rb/^{86}Sr$ ratio in sample ZYF62 was probably caused by hydrothermal alteration, therefore it will not be considered in following discussion. Sample ZYF25 is not included in the isochron of the basic rocks although it plots very close to this line.

The possible cause for the existence of two parallel isochrons could be different magma sources for the basic and intermediate rocks. However, sample ZYF14 (basalt) together with the intermediate rocks formed one isochron, and sample ZYF14 is similar to other basalt samples both in major and trace element geochemistry. This rules out the possibility that sample ZYF14 has a different magma source from the other basalts. Another possible reason could be contamination. Mixing of the 'primary' magma with continental material having a different age and isotopic nature could account for the two isochrons. This could also be the reason that the samples of the Permian volcanic rocks are largely scattered in the plot of $^{147}Sm/^{144}Nd$ vs. $^{143}Nd/^{144}Nd$ (Fig. 6b).

We adopt 270 Ma as the age of the Permian volcanic rocks to calculate the initial $^{87}Sr/^{86}Sr$ and ε_{Nd} values. The intermediate rocks generally have higher initial $^{87}Sr/^{86}Sr$ ratios (from 0.7051 to 0.7052, except sample ZYF62, which has an extremely low initial $^{87}Sr/^{86}Sr$ ratio of 0.70275) and lower ε_{Nd} values (from –0.73 to –3.57) than the basic rocks, which have initial $^{87}Sr/^{86}Sr$ ratios ranging from 0.7034 to 0.7051 and ε_{Nd} values from 2.72 to –0.10 (Table 1).

6. Discussion

6.a. Fractional crystallization

Fractional crystallization generally plays an important role in magma processes, especially in early stages and at depth (see the summary by Hawkesworth *et al.* 2000). Fractionation of diopside is evident from large variations in Mg no. and compatible trace elements (Fig. 3), and probably controls the compositions of major and compatible trace elements. The strong correlations between SiO_2 and other major elements (Fig. 2) suggest that fractional crystallization played

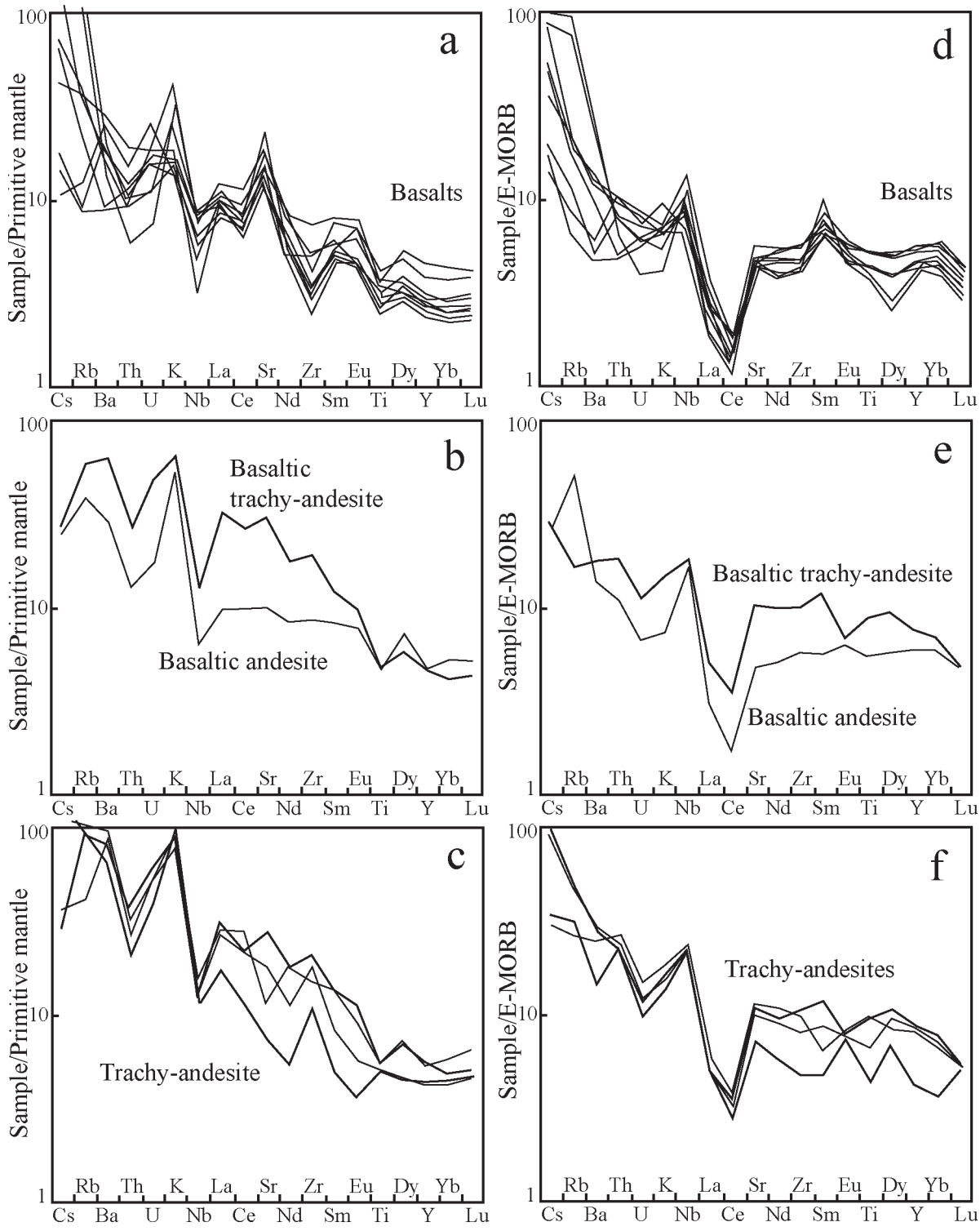

Figure 5. Primitive mantle-normalized multi-element diagrams for basalts (a), basaltic andesite and basaltic trachy-andesite (b) and trachy-andesites (c). E-MORB normalized diagrams (d–f) are shown for comparison. Both primitive mantle and E-MORB data are from Sun & McDonough (1989).

an important role in the Permian magma evolution. Diopside, occurring as phenocrysts, is important for the basic rocks. Plagioclase and amphibole become important for the more differentiated rocks. Diopside accumulation could account for high Fe_2O_3 and CaO contents in the basic rocks. Strong enrichment in TiO_2 combined with depletion in Fe_2O_3 with decreasing Mg no. from basic to intermediate rocks suggests little or no magnetite fractionation. TiO_2 contents therefore are not controlled by magnetite fractionation. Accumulation of amphibole can account for high TiO_2 and Al_2O_3 contents in the intermediate rocks

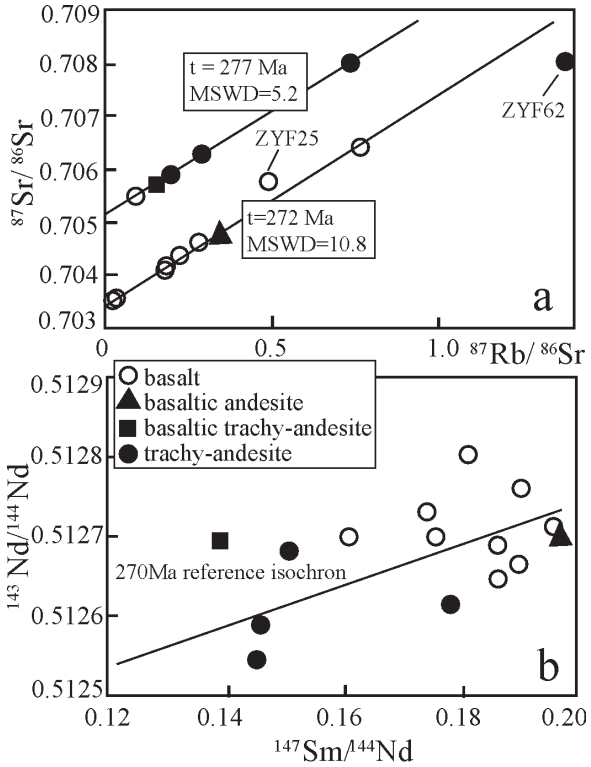

Figure 6. (a) Intermediate rocks (except ZYF62) and one basalt sample (ZYF14) form a Rb–Sr isochron giving an age of 277 ± 15 Ma with initial $^{87}Sr/^{86}Sr$ of 0.705107 ± 0.000066 (MSWD = 5.2). The basic rocks form another Rb–Sr isochron giving an age of 272 ± 11 Ma with initial $^{87}Sr/^{86}Sr$ of 0.703481 ± 0.000048 (MSWD = 10.8). (b) No isochron formed in the plot of $^{147}Sm/^{144}Nd$ vs. $^{143}Nd/^{144}Nd$. A 270 Ma reference isochron is drawn for comparison.

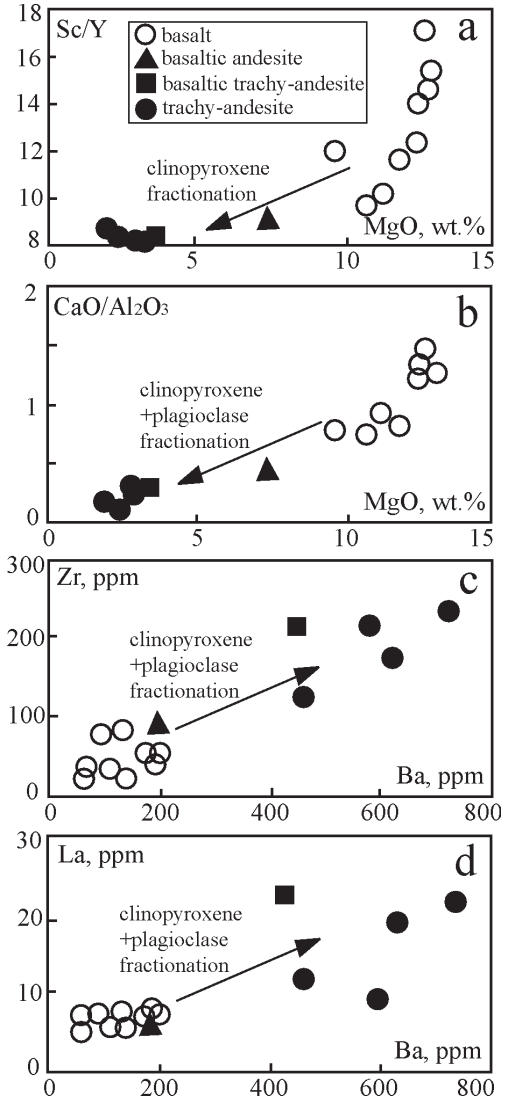

Figure 7. Plots of MgO vs. Sc/Y (a) and CaO/Al_2O_3 (b) show clinopyroxene (± plagioclase) fractionation trends. The clinopyroxene + plagioclase differentiation trend is shown in the plots of Ba vs. Zr (c) and La (d).

(Fig. 3a, b). Diopside fractionation is reflected in Figure 3c–d and in plots of MgO vs. Sc/Y and CaO/Al_2O_3 (Fig. 7a,b). As demonstrated by Naumann & Geist (1999), Sc/Y ratios are unaffected by olivine and plagioclase crystallization; lower ratios with decreasing MgO only reflects clinopyroxene fractionation. The fractionation of clinopyroxene + olivine + plagioclase can cause CaO/Al_2O_3 to increase with decreasing MgO contents. The linear arrays on plots of moderately incompatible Zr and very incompatible elements Ba and La (Fig. 7c,d) are consistent with the fractionation hypothesis (e.g. Hanson, 1989). However, samples of the intermediate rocks are relatively scattered in these plots, which suggests that some other processes are required besides the fractionation crystallization.

If only fractional crystallization occurred, Sr and Nd isotope ratios should be constant with variations of Mg no. and incompatible trace elements. The differences in Sr–Nd isotope ratios (Fig. 6) and Mg no. (Fig. 3a–d) as well as the existence of two parallel Rb–Sr isochrons (Fig. 6a) cannot be explained by fractional crystallization. This therefore strongly suggests the existence of different sources for the Permian magma.

6.b. Assimilation of continental crust

The differences between the Sr and Nd isotope compositions of the basic and intermediate rocks rule out one origin of each whole assemblage by simple fractional crystallization and strongly support the occurrence of open-system processes. The presence of continental crust was thought to be a fundamental requirement for the formation of calc-alkaline magma in orogenic volcanic associations (Coulon & Thorpe, 1981). Ratios of highly incompatible elements (Ba, U, Th, Nb, La, Sm) will not be fractionated greatly during partial melting, and these ratios have been shown to be unaffected by partial melting processes in the mantle (Hofmann, 1988). These ratios have vastly different values in oceanic magmas and continental magmas. Thus, variation of these ratios in volcanic

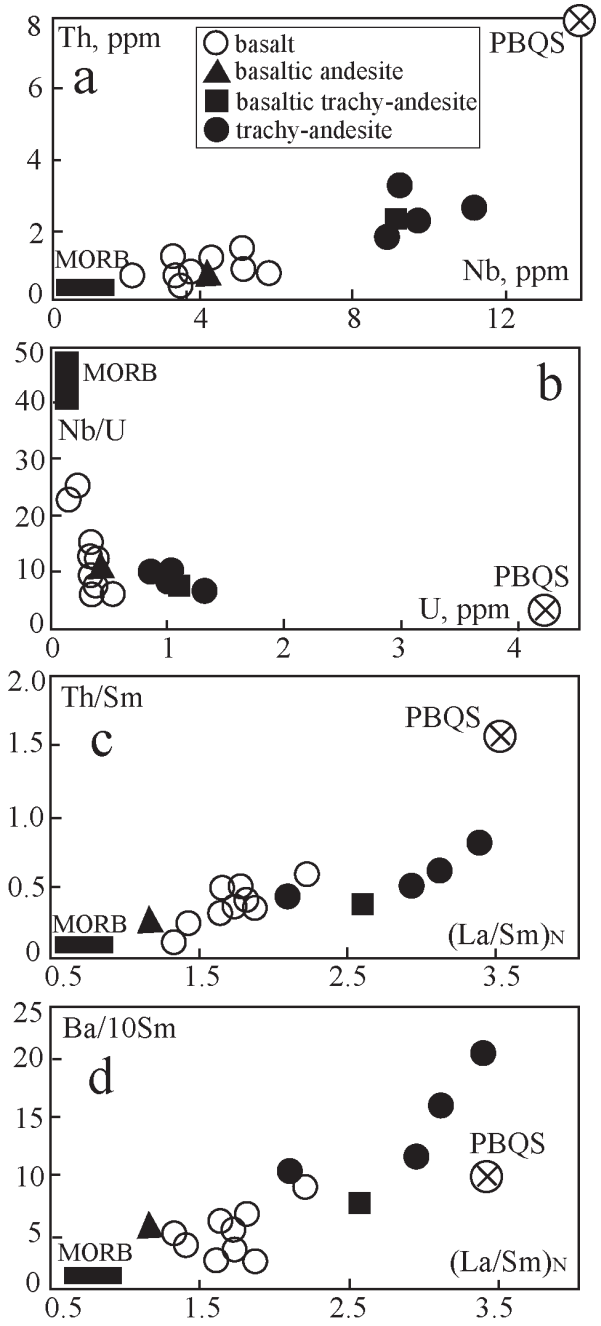

Figure 8. Plots of Th vs. Nb (a), Nb/U vs. U (b), Th/Sm (c) and Ba/Sm (d) ratios vs. chondrite normalized La/Sm ratio for the Permian volcanic rocks. Values for MORB and Proterozoic biotite–quartz schist (PBQS) in Mongolia are marked for comparison. MORB and chondrite values are taken from Sun & McDonough (1989).

rocks can provide information about the effect of continental material in magma sources.

Pelagic sediments are highly enriched in Th (e.g. Ben Othman, White & Patchett, 1989), and Th and Nb are considered to be immobile elements in subduction-derived fluids (Plank, 1996; Keppler, 1996). Both Th and Nb are highly incompatible and their contents should therefore be unaffected by magmatic differentiation. The strong positive correlation between Nb and Th from the basic to intermediate rocks (Fig. 8a) suggests that the intermediate rocks have been strongly affected by continental material relative to the basic rocks.

In contrast to the immobile behaviour of Th and Nb, U is relatively mobile in fluids (Pearce & Parkinson, 1993; Hoernle, 1998). U-enrichment caused by fluid may account for the low Nb/U ratios of the Permian volcanic rocks (Fig. 8b). All samples have Nb/U ratios lower than MORB average values and most of them are close to the continental crust values. The high U concentrations in the intermediate rocks (0.86–1.30 ppm, Table 1) suggest that the intermediate rocks must have received additional U from continental material. The assimilation of Proterozoic biotite–quartz schist may also be a good explanation for U enrichment, as the Proterozoic biotite–quartz schist has a rather high U content (4.13 ppm, Table 1).

The correlation between the $(La/Sm)_N$ and Th/Sm ratios (Fig. 8c) suggests that LREE enrichment and sediment addition are directly related. LREE enrichment is also accompanied by increasing Ba/Sm ratios, shown in the plot of $(La/Sm)_N$ vs. Ba/Sm (Fig. 8d). However, Ba/Sm ratios of some intermediate rocks are even higher than those from the Proterozoic biotite–quartz schist. This can be explained in the following three ways: (1) fluid caused Ba enrichment, as Ba is a fluid-mobile element; (2) small amounts of contamination could explain why Ba shows an order of magnitude greater variation in continental volcanic rocks than do many other elements (DePaolo, 1981); and (3) an extremely low degree of partial melting can cause Ba enrichment in the melt because Ba is a highly incompatible element.

Highly variable Sr–Nd isotope ratios are a characteristic of continental basalts due to the additional isotopic heterogeneity derived from the continental crust or the lithospheric mantle (Ellam & Stuart, 2000). In a plot of ε_{Nd} vs. initial $^{87}Sr/^{86}Sr$ (Fig. 9) the basic rocks are characterized by high ε_{Nd} and low initial $^{87}Sr/^{86}Sr$ values, and the intermediate rocks have relatively low but highly variable ε_{Nd} values with high initial $^{87}Sr/^{86}Sr$ ratios. The assimilation fractional crystallization (DePaolo, 1981) model is used to explain these isotope characteristics. In the assimilation fractional crystallization calculations, F represents the ratio of residual magma mass to the initial magma mass. The lower the value of F the greater the fractional crystallization. The value of r represents the ratio of assimilated wall-rock to the rate at which fractionating phases are being effectively separated from the magma. The larger the r values the stronger the assimilation process. This value may be changing continuously as magma moves through the continental crust. D_{Sr} and D_{Nd} represent the bulk solid/liquid partition coefficient between the fractionating crystalline phases and the magma for Sr and Nd, respectively. In all probability as magma moves through the continental crust, D_{Sr} may be

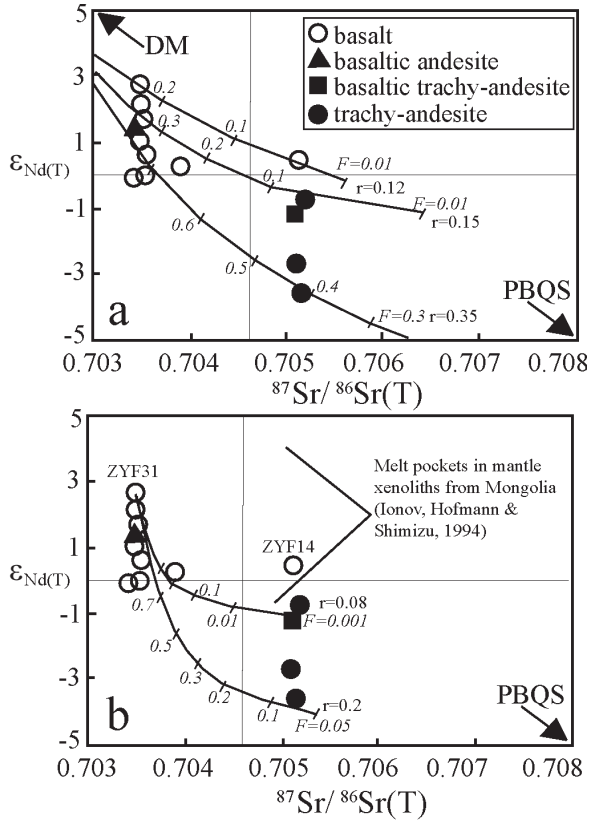

Figure 9. Initial $^{87}Sr/^{86}Sr$ vs. ε_{Nd} for the Permian volcanic rocks. Calculation shows assimilation combined with fractional crystallization between the Proterozoic biotite–quartz schist (PBQS) and two different 'primary' magmas as represented by (a) clinopyroxene in mantle xenolith (DM), and (b) the least contaminated basalt sample ZYF31. See text for details.

changing continuously. Under conditions in which plagioclase is unlikely to be the major fractionating phase, the D_{Sr} values are likely to be less than one (DePaolo, 1981). As the magma moves up through the crust it will encounter cooler wall-rocks and the heat budget of the system will work to inhibit assimilation and accelerate crystallization; consequently, the value of *r* will decrease, and as differentiation proceeds, plagioclase will become the dominant fractionating phase (Wyllie, 1979) and D_{Sr} will increase. Based on the distribution coefficients of Sr and Nd (cf. Rollinson, 1993, for a summary of distribution coefficients) and the mineral phases of the Permian volcanic rocks, D_{Sr} = 1 and D_{Nd} = 0.2 were used in the assimilation fractional crystallization calculations.

The nature of the subcontinental mantle under the studied area, which corresponds to the Permian magma source, is not clear. Different 'primary' magmas are therefore assumed in the assimilation fractional crystallization calculations. The Mongolian subcontinental mantle can be represented by the clinopyroxene in a mantle xenolith (average ε_{Nd} = 9.3, Nd = 4.51 ppm; the lowest initial $^{87}Sr/^{86}Sr$ = 0.702, Sr = 88.5 ppm; Stosch, Lugmair & Kovalenko, 1986). The compositions of the Permian volcanic rocks can be modelled by the assimilation fractional crystallization processes with end-members of this mantle and the Proterozoic biotite–quartz schist (Fig. 9a) at reasonable values of *r* (0.12–0.35) and *F* (0.05–0.75).

When the least contaminated basalt sample ZYF31 is used as a primary magma, the assimilation fractional crystallization calculations could possibly reproduce some of the Permian volcanic rocks with *r* = 0.08–0.2 and *F* = 0.001–0.9 (Fig. 9b). However, the other samples cannot be modelled. This suggests that the least contaminated rock sample cannot represent the source magma. The original magma must be heterogeneous or have experienced fractional crystallization or contamination. Melt pockets in the metasomatized mantle xenolith from central Mongolia (Ionov, Hofmann & Shimizu, 1994) are shown in this plot for comparison. Their ε_{Nd} values have relatively large variations although their Sr isotope ratios change little. It is evident from this plot that the data sets of these melt pockets cannot produce the Permian volcanic rocks by the assimilation fractional crystallization processes with the Proterozoic biotite–quartz schist.

6.c. Magma sources

Numerous studies (e.g. Stolper & Newman, 1994; Keppler, 1996) have demonstrated that the budget of LILE in magma is controlled by fluid influx, whereas the budgets of the incompatible trace elements including heavy REE (HREE) and high field strength elements (HFSE: Nb, Zr, Y, Ti) are controlled by partial melting processes and mantle depletion. HREE and HFSE are thus preferred here to constrain the composition of magma sources. The production of magma in an orogenic zone may involve a large number of components including MORB, OIB, subduction sediments and oceanic crust. The origin of subduction-related magma is a multi-stage, multi-component and multi-process geological event (e.g. Di Vincenzo & Rocchi, 1999). The complexity and variation of isotope compositions and trace element abundances suggest that the formation of the Permian volcanic rocks may involve complex magma sources or processes of crust contamination.

Garnet has a high partition coefficient for Y ($D_{garnet/melt}$ = 4–11: Jenner *et al.* 1994) relative to Zr ($D_{garnet/melt}$ = 0.4–0.7: Jenner *et al.* 1994). Varying amounts of residual garnet in the sources would change the Y contents in the magmas and Zr/Y would correlate with Y. In the Permian volcanic rocks Zr/Y ratios are strongly correlated with Zr contents (Fig. 10a), but not with Y contents (Fig. 10b). This indicates that there is no residual garnet in the magma sources. In such a case, contribution of the 'excess' Zr to the mantle source is required as shown by the source enrichment direction in Figure 10b, either from an

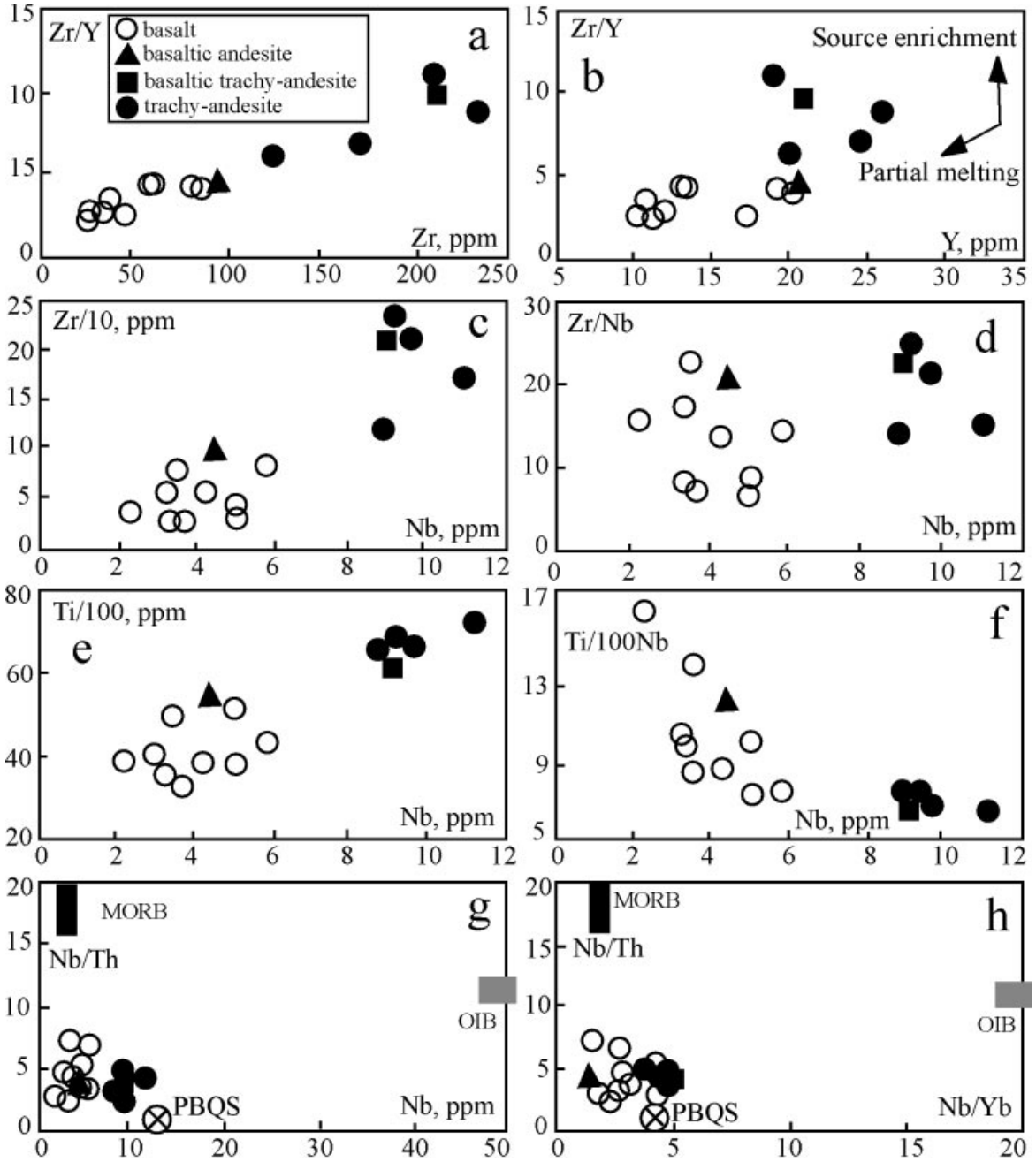

Figure 10. Plots for high field strength elements and their ratios for the Permian volcanic rocks. See text for details. PBQS = Proterozoic biotite–quartz schist.

OIB source or from the continental material (subduction sediments). Nb is extremely sensitive to depletion events because it enters the melt very efficiently; Nb is strongly correlated with Zr and Ti in the Permian volcanic rocks, with higher concentrations in the intermediate rocks than in the basic rocks (Fig. 10c,e). However, the Nb contents do not correlate with Zr/Nb ratios (Fig. 10d). The Zr/Nb ratios are highly variable and almost equal for the intermediate and basic rocks. The Ti/Nb ratios correlate with Nb contents, with Nb increasing as the Ti/Nb values decrease drastically (Fig. 10f). These observations suggest that the Zr contents are slightly higher relative to Nb contents, especially in the intermediate rocks, but Ti is depleted relative to Nb in the intermediate rocks. Therefore, as with Zr, addition of Nb to the magma source is required. An OIB mantle and/or subduction sediments could be the sources of these trace elements.

Although high Nb content has been used as major evidence for an OIB component in the magma source (e.g. Edwards *et al.* 1994), the addition of melts derived from continental sediments can also add Nb to magma (Stolz et al. 1996; Hoogewerff *et al.* 1997). The Nb content is positively correlated with Th abundances (Fig. 8a), but not with Nb/Th ratios (Fig. 10g). This suggests that the increase of Nb content in the

magma is accompanied by increasing Th content, and therefore both Nb and Th are added from other sources. The Nb/Th ratios in the Permian volcanic rocks do not correlate with Nb/Yb ratios (Fig. 10h). Any significant role of OIB in the source can be ruled out, as suggested by Munker (2000), since a correlation of Nb/Th with Nb/Yb would be expected in the case of mixing between MORB and OIB source mantle.

Therefore, only two components are required in the Permian magma source: a MORB mantle source and subducted continental sediments. The MORB mantle source is consistent with most REE and HFSE abundances in the Permian volcanic rocks (Fig. 5d–f). These two end-members are also consistent with the tectonic setting of this region. A continental collision caused by the subduction of oceanic crust occurred before the Permian volcanism. The final collision should not have been earlier than 310 Ma as shown by the age of the arc granitoids (Chen *et al.* 2000) located in the west close to the studied area. Therefore, there was a subduction slab in the mantle prior to Permian volcanism, and the slab should contain some continental sediments.

6.d. The recycling of oceanic crust

LILE contents are usually high in continental crust and can therefore be used as an indicator of crustal assimilation. LILE concentrations could be controlled by subduction-derived fluid, which can cause mantle metasomatism (e.g. McCulloch & Gamble, 1991). The high LILE content of the Permian volcanic rocks (Fig. 5) therefore may suggest an additional 'crust + fluid' component. The intermediate rocks are especially enriched in Ba (mostly higher than 400 ppm) relative to the basic rocks (less than 200 ppm, Table 1). This indicates that the intermediate rocks were modified by fluid with higher concentrations of LILE relative to the basic rocks.

Strong positive Sr anomalies in the primitive mantle-normalized diagram are the main features of the basic rocks (Fig. 5a). Plagioclase melting in the source region could be one reason for the Sr enrichment, as a Sr-rich signature has been taken as evidence for absence of plagioclase in the melting residue (Defant & Drummond, 1990). The intermediate rocks have largely variable Sr contents and show no Sr peaks in the primitive mantle-normalized diagrams (Fig. 5c). One reason for this is the fractionation of plagioclase, which is proved by the occurrence of plagioclase phenocrysts. The Proterozoic biotite–quartz schist could not supply abundant Sr during the assimilation fractional crystallization process because of the low Sr content (about 100 ppm). The high mobility of Sr relative to less mobile trace elements could be the reason for the Sr-rich feature, as suggested by Pearce (1983). Significant loss of Sr in slab sediments during early dehydration of the slab would lead to Sr enrichment in the mantle. This process would cause other LILE enrichments in the mantle. Even though a low degree of partial melting could cause high LILE concentrations in the magma, the degree of partial melting could not be very low as there is no residual garnet in the magma sources. A subduction component with high LILE concentrations is therefore required to explain the LILE enrichments in the Permian volcanic rocks.

The rocks with low ε_{Nd} and high initial $^{87}Sr/^{86}Sr$ values could have been produced by a combination of continental crust and mantle as suggested by many authors (e.g. Hart, 1988; Hofmann, 1997; Peccerillo, 1999). Altered oceanic crust mixing with subcontinental mantle can produce magma with low ε_{Nd} and high initial $^{87}Sr/^{86}Sr$ values, so the recycling of altered oceanic crust is a plausible source for the Permian volcanic rocks in the Mongolian orogenic zone. The recycling of oceanic lithosphere has attracted much attention in recent years (e.g. Hoernle, 1998; Hildebrand & Bowring, 1999; Hauff *et al.* 2000). These authors suggested that the average recycled oceanic lithosphere could have formed within 200–500 Ma before the basalt event, and mantle plume heads could facilitate the recycling of large volumes of oceanic lithosphere within a few hundred million years. As the collision events in the Mongolian orogenic zone took place later than 310 Ma (the age of the arc granitoid) and the oceanic crust formed at 430 Ma (the age of the Hegenshan ophiolite), the oceanic crust must have returned into the mantle in about 120 Ma. We conjecture that the subduction slab stayed in the mantle for more than 40 Ma before it rose to surface at 270 Ma in the form of magma eruption.

7. Conclusions

Based on the chemical and Sr–Nd isotope compositions of the Permian volcanic rocks in the Mongolian orogenic zone, we propose that the subduction slab dropped into the depleted mantle and released fluid. This fluid induced mantle metasomatism and LILE enrichment, as fluids derived from subduction slabs generally contain considerable H_2O, SiO_2, LILE and LREE with low ε_{Nd} and high $^{87}Sr/^{86}Sr$ initial values (e.g. El Bakkali *et al.* 1998). Afterwards, the metasomatized mantle partially melted and formed the 'primary' magma. This primary magma assimilated with the Proterozoic biotite–quartz schist during its rise, and finally formed the Permian volcanic rocks. The magma assimilated with the Proterozoic biotite–quartz schist in small amounts could have produced the basic rocks, while assimilation of larger amounts of magma (because of longer assimilation time) would generate intermediate rocks. Subduction of the slab into the mantle is therefore the key factor in the Permian volcanism in the Mongolian orogenic zone.

The thermal and weight instability of the slab and its released fluids are the main reasons for the volcanism. Volcanism probably was triggered as part of the regional response to extension, which resulted in asthenospheric upwelling as documented by the geochemistry of Mesozoic intrusive bodies (Shao, Gai & Zhang, 1998).

Acknowledgements. The authors thank Dr Jianghai Li and Baofu Han (Peking Univ.) for their fruitful comments, Heping Zhu and Xindi Jin for their aid in the ICP-MS laboratory work, Chaofeng Li for his aid in the Finnigan MAT 262 laboratory work. Thoughtful and detailed reviews by Dr Jean-Paul Liegeois, Dr Rob Ellam and an anonymous referee helped to improve this manuscript greatly. This work has been financially supported by the Chinese Academy of Science (project KZ-951-B1-404) and NSFC (No. 49673193).

References

Ben Othman, D., White, W. M. & Patchett, J. 1989. The geochemistry of marine sediments, island arc magma genesis, and crust-mantle recycling. *Earth and Planetary Science Letters* **94**, 1–21.

Chen, B., Jahn, B., Wilde, S. & Xu, B. 2000. Two contrasting Paleozoic magmatic belts in northern Inner Mongolia, China: petrogenesis and tectonic implications. *Tectonophysics* **328**, 157–82.

Coulon, C. & Thorpe, R. 1981. Role of continental crust in petrogenesis of orogenic volcanic associations. *Tectonophysics* **77**, 79–93.

Defant, M. J. & Drummond, M. S. 1990. Derivation of some modern arc magmas by melting of young subducted lithosphere. *Nature* **347**, 662–5.

DePaolo, D. J. 1981. Trace elements and isotopic effects of combined wallrock assimilation and fractional crystallization. *Earth and Planetary Science Letters* **53**, 189–202.

Di Vincenzo, G. & Rocchi, S. 1999. Origin and interaction of mafic and felsic magmas in an evolving late orogenic setting: the Early Paleozoic Terra Nova intrusive complex, Antarctica. *Contributions to Mineralogy and Petrology* **137**, 15–35.

Edwards, C. M. H., Menzies, M. A., Thirlwall, M. F., Morris, J. D., Leeman, W. P. & Harmon, R. S. 1994. The transition to potassic alkaline volcanism in island arcs: the Ringgit-Beser complex, east Java, Indonesia. *Journal of Petrology* **35**, 1557–95.

El Bakkali, S., Gourgaud, A., Bourdier, J. L., Bellon, H. & Gundogdu, N. 1998. Post-collision neogene volcanism of the Eastern Rif (Morocco): magmatic evolution through time. *Lithos* **45**, 523–43.

Ellam, R. M. & Stuart, F. M. 2000. The sub-lithospheric source of North Atlantic basalts. Evidence for, and significance of, a common end-member. *Journal of Petrology* **41**, 919–31.

Hanson, G. N. 1989. An approach to trace element modeling using a simple igneous system. *Reviews in Mineralogy* **21**, 79–97.

Hart, S. R. 1988. Heterogeneous mantle domains: signatures, genesis and mixing chronologies. *Earth and Planetary Science Letters* **90**, 273–96.

Hauff, F., Hoernle, K., Tilton, G., Graham, D. W. & Kerr, A. C. 2000. Large volume recycling of oceanic lithosphere over short time scales: geochemical constraints from the Caribbean Large Igneous Province. *Earth and Planetary Science Letters* **174**, 247–63.

Hawkesworth, C. J., Blake, S., Evans, P., Hughes, R., Macdonald, R., Thomas, L. E., Turner, S. P. & Zellmer, G. 2000. Time scales of crystal fractionation in magma chambers – Integrating physical, isotopic and geochemical perspectives. *Journal of Petrology* **41**, 991–1006.

Hildebrand, R. S. & Bowring, S. A. 1999. Crustal recycling by slab failure. *Geology* **27**, 11–14.

Hoernle, K. 1998. Geochemistry of Jurassic oceanic crust beneath Gran Canaria (Canary Islands): Implications for crustal recycling and assimilation. *Journal of Petrology* **39**, 859–80.

Hofmann, A. W. 1988. Chemical differentiation of the Earth: the relationship between mantle, continental crust and oceanic crust. *Earth and Planetary Science Letters* **90**, 297–314.

Hofmann, A. W. 1997. Mantle geochemistry: the message from oceanic volcanism. *Nature* **385**, 219–29.

Hoogewerff, J. A., van Bergen, M. J., Vroon, P. Z., Hertogen, J., Wordel, R., Sneyers, A., Nasution, A., Varekamp, J. C., Moens, H. L. E. & Mouchel, D. 1997. U-series, Sr–Nd–Pb isotope and trace-element systematics across an active island arc–continent collision zone: implications for element transfer at the slab–wedge interface. *Geochimica et Cosmochimica Acta* **61**, 1067–72.

Hsu, K. J., Wang, Q. & Hao, J. 1991. Geologic evolution of the Neomonides: a working hypothesis. *Eclogae Geologicae Helvatiae* **84**, 1–31.

Ionov, D. A., Hofmann, A. W. & Shimizu, N. 1994. Metasomatism-induced melting in mantle xenoliths from Mongolia. *Journal of Petrology* **35**, 753–85.

Jenner, G. A., Foley, S. F., Jackson, S. E., Green, T. H., Fryer, B. J. & Longerich, H. P. 1994. Determination of partition coefficients for trace elements in high pressure–temperature experimental run products by laser ablation microprobe-inductively coupled plasmamass spectrometry (LAM-ICP-MS). *Geochimica et Cosmochimica Acta* **58**, 5099–5130.

Keppler, H. 1996. Constraints from partitioning experiments on the composition of subduction-zone fluids. *Nature* **380**, 237–40.

Le Maitre, R. W., Bateman, P., Dudek, A., Keller, J., Lameyre, J., Le Bas, M. J., Sabine, P. A., Schmid, R., Sorensen, H., Streckeisen, A., Woolley, A. R. & Zanettin, B. 1989. *A classification of igneous rocks and glossary of terms*. Oxford: Blackwell.

Liegeois, J. P. 1998. Preface – some words on the post-collisional magmatism. *Lithos* **45**, ix–xii.

Liegeois, J. P., Navez, J., Hertogen, J. & Black, R. 1998. Contrasting origin of post-collisional high-K calc-alkaline and shoshonitic versus alkaline and peralkaline granitoids. The use of sliding normalization. *Lithos* **45**, 1–28.

Ludwig, K. R. 2000. *Isoplot/Ex version 2.3. A geochronological toolkit for Microsoft Excel*. Berkeley Geochronology Center Special Publication no. 1a, pp. 1–54.

McCulloch, M. T. & Gamble, J. A. 1991. Geochemical and geodynamical constraints on subduction zone magmatism. *Earth and Planetary Science Letters* **102**, 358–74.

Munker, C. 2000. The isotope and trace element budget of the Cambrian Devil River Arc system, New Zealand:

identification of four source components. *Journal of Petrology* **41**, 759–88.

Naumann, T. R. & Geist, D. J. 1999. Generation of alkalic basalt by crystal fractionation of tholeiitic magma. *Geology* **27**, 423–6.

Pearce, J. A. 1983. Role of the sub-continental lithosphere in magma genesis at active continental margins. In *Continental basalts and mantle xenoliths* (eds C.J. Hawkesworth and M.J. Norry), pp. 230–49. Nantwich: Shiva.

Pearce, J. A. & Parkinson, I. J. 1993. Trace element models for mantle melting: application to volcanic arc petrogenesis. In *Magmatic processes and plate tectonics* (eds H. M. Prichard, T. Alabaster, N. B. W. Harris and C. R. Neary), pp. 373–403. Geological Society of London, Special Publication no. 76.

Peccerillo, A. 1999. Multiple mantle metasomatism in central-southern Italy: geochemical effects, timing and geodynamic implications. *Geology* **27**, 315–18.

Plank, T. 1996. The brine of the Earth. *Nature* **380**, 202–3.

Robinson, P., Zhou, M. F., Hu, X. F., Reynold, P., Bai, W. J. & Yang, J. S. 1999. Geochemical constraints on the origin of the Hegenshan ophiolite, Inner Mongolia, China. *Journal of Asian Earth Sciences* **17**, 423–42.

Rollinson, H. 1993. *Using geochemical data; evolution, presentation, interpretation*. New York: Longman Scientific & Technical, 352 pp.

Sengor, A. M. C. & Natal'in, B. A. 1996. Paleotectonics of Asia: fragments of a synthesis. In *The tectonic evolution of Asia* (eds A. Yin and T. M. Harrison), pp. 486–640. Cambridge University Press.

Sengor , A. M. C., Natal'in, B. A. & Burtman, V. S. 1993. Evolution of the Altaid tectonic collage and Palaeozoic crustal growth in Eurasia. *Nature* **364**, 299–307.

Shao, Ji'an. 1991. *Crust evolution in the middle part of the northern margin of Sino-Korean plate*. Beijing: Peking University Publishing House, 136 pp.

Shao, Ji'an, Gai, F. & Zhang, L. 1998. Coupling of mantle-upwelling and shearing – Mesozoic dyke-swarms in Da-Hinggan mountains, Northeast China. *Episodes* **21**, 99–103.

Stolper, E. & Newman, S. 1994. The role of water in the petrogenesis of the Mariana trough magmas. *Earth and Planetary Science Letters* **121**, 293–325.

Stolz, A. J., Jochum, K. P., Spettel, B. & Hofmann, A. W. 1996. Fluid and melt related enrichment in the subarc mantle: evidence from Nb/Ta variations in island arc basalts. *Geology* **24**, 587–90.

Stosch, H. G., Lugmair, G. W. & Kovalenko, V. I. 1986. Spinel peridotite xenoliths from the Tariat Depression, Mongolia. II: Geochemistry and Nd and Sr isotopic compositions and implications for the evolution of the subcontinental lithosphere. *Geochimica et Cosmochimica Acta* **50**, 2601–14.

Sun, S. S. & McDonough, W. F. 1989. Chemical and isotope systematics of oceanic basalts: implications for mantle composition and processes. In *Magmatism in the ocean basins* (eds A. D. Saunders and M. J. Norry), pp. 313–45. Geological Society of London, Special Publication no. 42.

Tang, K. D. 1990. Tectonic development of Paleozoic foldbelts at the north margin of the Sino-Korean craton. *Tectonics* **9**, 249–60.

Wyllie, P. J. 1979. Magmas and volatile components. *American Mineralogist* **64**, 469.

Zorin, Yu. A., Belichenko, V. G. & Turutano, E. K. 1993. The south Siberian-central Mongolia transect. *Tectonophysics* **225**, 361–78.